

# Surface Effect of Laser Power on Microstructural Evolution and Hardness Behaviour of Titanium Matrix Composites

Musibau O. Ogunlana and Esther T. Akinlabi, *Member, IAENG*

**Abstract**—In this paper, Titanium alloy (Ti6Al4V) powder and boron carbide (B<sub>4</sub>C) powder metal matrix composites (MMCs) were embedded on titanium alloy (Ti6Al4V) substrate using laser metal deposition (LMD). The laser power was varied between 800 W and 2400 W at an interval of 200 W while all other processing parameters were kept constant. The maximum capacity of the laser system is 3.0 KW which provides beam size of 4 mm for the control characterization of the deposited samples. The microstructural properties of the deposited samples were profound with  $\alpha$  and  $\beta$  (intermetallic phase of  $\alpha+\beta$ ) of titanium alloy and boron carbide particles. The optical microscope (OM) was employed to characterise the grain sizes and microstructures. The microhardness were characterized using the Vickers' hardness indenter in which the microhardness of the composites revealed an increase in the samples as the laser power increases. The hardness were observed to be between 371Hv and 471Hv for the clad samples when compared to the substrate with approximately 360Hv.

**Index Terms**—Boron Carbide, Laser Metal Deposition, Laser Power, Microhardness, Microstructure, Metal Matrix Composites, Titanium alloy

## I. INTRODUCTION

TITANIUM and its alloys are used for highly demanding applications such as in the fabrication of some of the most critical and highly stressed civilian and military aircraft parts, chemical processing, automobile industries, nuclear power plants, food processing plants and oil refinery heat exchangers. This wide range of applications have been attributed to its excellent properties such as low density, high specific strength, heat resistance, corrosion resistance, low temperature resistance and excellent biocompatibility. Suggestions have been made that the physical and mechanical properties of titanium can be improved through the incorporation of reinforcing compounds using the principle of metal matrix composites (MMCs). This is because MMCs combine the properties of ceramics and

metals to produce materials with attractive properties like good shear strength, high temperature strength and elevated hardness [1]. On the other hand, [2] researched on laser metal deposition (LMD) as an additive manufacturing (AM) technique which serves as a recommended technique for processing titanium and its alloy because it addresses most of the problems of the traditional manufacturing methods simply because AM technique is a tool-less process.

However, [3] also researched that AM technology is a promising aerospace manufacturing technique as it has the potential of reducing the buy-to-fly ratio and it is useful for the repair of high valued parts. There are various methods for coating surfaces of materials, some of them includes chemical vapour deposition, physical vapour deposition, spraying, etc. but the laser metal deposition (LMD) process, is an additive manufacturing process and it is believed to have a greater advantage when compared to other deposition processes. Some of the advantages of using the LMD process include the ability to produce parts directly from the 3-Dimensional (3D) computer aided design (CAD) model of the part with the required surface coating in one single step, as against only coating achievable with other surface coating techniques. Another important advantage of the LMD process is in its ability to be used to repair existing worn out parts that were not repairable in the past. Also, complex parts can be produced with the LMD without requiring later assembly, since the part can be made as one single component, this will greatly reduce the buy-to-fly ratio of aerospace parts [4]-[6].

Laser beams are widely used in surface modification of different metals, owing to their high coherence, directionality and high energy density. Furthermore, laser surface remelting, laser alloying, and laser cladding have been researched by [7] to improve the surface properties of many kinds of metals. It is noteworthy that the coatings prepared by laser cladding show dense microstructure and exhibit strong metallurgical bonding with the substrates. Furthermore, boron carbide (B<sub>4</sub>C) has considerably properties such as: a high melting point, outstanding hardness, good mechanical properties, low specific weight and great resistance to chemical agents, is currently used in high-technology industries fast-breeders, lightweight armours and high temperature thermoelectric conversion. In the group of the most important non-metallic hard materials (alumina, silicon carbide, silicon nitride, diamond or cubic boron nitride), boron carbide occupies a specific place. A boron carbide compound was discovered in 1858, and then Joly in 1883 and Moissan in 1894. These compounds were

Manuscript received February 29, 2016; revised March 10, 2016.

Musibau O. Ogunlana is a Masters Candidate in the Department of Mechanical Engineering Science, University of Johannesburg, Auckland Park Kingsway Campus, Johannesburg, South Africa, 2006. (E-mail: 201510083@student.uj.ac.za or [emmbbyola@gmail.com](mailto:emmbbyola@gmail.com)).

Prof Esther T. Akinlabi is an Associate Professor and the Head of Department in the Department of Mechanical Engineering Science, University of Johannesburg, Auckland Park Kingsway Campus, Johannesburg, South Africa, 2006. Phone: +2711-559-2137, (E-mail: [etakinlabi@uj.ac.za](mailto:etakinlabi@uj.ac.za)).

prepared and identified as  $B_3C$  and  $B_6C$ , respectively. The 'stoichiometric formula'  $B_4C$  was only assigned in 1934, and then many diverse formulae were proposed by the Russian authors. After 1950, numerous studies were carried out, especially concerning structures and properties of boron carbide [8].

Boron carbide is an extremely promising material for a variety of applications that require elevated hardness, good wear and corrosion resistance [9]. Application of boron carbide,  $B_4C$  in the highlighted areas is due to its excellent properties that include high hardness, high wear resistance, high melting point and high thermal conductivity. This material is reported as the third hardest (after diamond and cubic boron nitride) of the technically useful materials. Boron carbide,  $B_4C$  currently finds application in the nuclear industry and high-temperature thermo-electric conversion but there is restriction to its wide industrial application because of low strength (about 200 - 400MPa), low fracture toughness ( $2-3 \text{ MPa}\cdot\text{m}^{0.5}$ ), as well as poor sinterability that results from its low self-diffusion coefficient. Grain refined boron modified Ti6Al4V alloy has shown significant improvement in strength, stiffness, fatigue resistance and fracture toughness. However, researchers showed the enhanced formability of boron modified alloy during large deformation without cracking as oppose to the normal alloy.

Owing to the fact that microstructural evolution during hot deformation has an important influence on the mechanical properties of the final product, understanding the processing-microstructure relationship during thermo-mechanical processing of boron modified Ti6Al4V is of great importance [10], [11]. The surface effect of sample composites using the laser power as the commanding parameter on the microstructure and the microhardness of Ti6Al4V- $B_4C$  were carefully investigated in this study while keeping the scanning speed, the powder flow rate and gas flow rate constant throughout the experiments.

## II. EXPERIMENTAL PROCEDURE

The experimental materials involved in this study are Ti6Al4V powder produced by Alfa Aesar Company and  $B_4C$  powder also supplied by the same company in Germany. The laser metal deposition (LMD) process was achieved with 3.0 KW Ytterbium fibre laser system with coaxial powder nozzles. A Kuka robot was used to carry both the laser and powder nozzles and also controls the deposition process. The rectangular Ti6Al4V substrate with dimensions 102 mm x 102 mm x 7 mm is prepared for the laser metal deposition of the mixture powders. Ti6Al4V alloy samples were sandblasted and cleaned under tap water and then dried with acetone prior to the coating operation. Boron carbide,  $B_4C$  powder with particle size of about 22-59  $\mu\text{m}$ , and the titanium alloy powder with particle size of 45-90  $\mu\text{m}$ , were deposited in the ratio of 1:4 in weight percent. The laser power used were varied between 800 W to 2400 W with 200 W interval. The beam diameter or spot size of 4mm was employed to melt the surface of the samples in which 12 mm focal distance was maintained from the nozzle to the surface of the substrate. During the laser surface

melting process, the powders were dissolved into the melted pool, leading to alloying the surface of the samples with boron carbide. To protect the melt pool from oxidation during laser deposition process, argon gas was initiated at a pressure of 2 MPa to provide shielding. The powders were fed through a nozzle which was coaxial with the laser beam.

Furthermore, the properties of Titanium alloy, Ti6Al4V used as substrate and as well as powder are described as follows: The substrate contains titanium alloy of Ti6Al4V with dimensions as 102mm x 102mm x 7mm while the powder contains properties with particle size range between 45 and 90  $\mu\text{m}$  (micron), spherical particle and 99.6 % purity. The mechanical properties of Ti6Al4V through forged then annealed is as follows: yield tensile strength 880 MPa, ultimate tensile strength 950 MPa, hardness (Hv) 349, young's modulus 113.8 GPa, Poisson's ratio 0.342, fracture toughness  $75 \text{ MPa}\cdot\text{m}^{0.5}$ .

However, the properties of boron carbide powder as-received are given as follow: density of  $> 2.48 \text{ g/cm}^3$ , porosity of  $< 0.5 \%$ , average particle size of  $< 15 \mu\text{m}$ , Vickers hardness of 31 GPa, knoop hardness of 29 GPa, elasticity of 420 GPa, Weibull modulus of 15m, flexural strength of 450 MPa, compression strength of  $> 2800 \text{ MPa}$ , poisson number of 0.15, fracture toughness of  $5 \text{ MPa}\cdot\text{m}^{0.5}$ , coefficient of thermal expansion at 20  $^\circ\text{C}$  is  $4.5 \times 10^{-6}/\text{K}$ , specific heat at 20  $^\circ\text{C}$  is 1 J/gK, thermal conductivity at 20  $^\circ\text{C}$  is 40 W/mK, specific electrical resistance at 20  $^\circ\text{C}$  is 1  $\Omega\text{cm}$  and purity of  $> 99\%$ . The photograph of the experimental set-up for the laser metal deposition process is shown in the Figure 1.



Fig. 1: Experimental set-up

The gas assisted powder was delivered into the melt pool created by the laser on the substrate in order to generate a deposited track. The schematic of the deposition process is shown in Figure 2. A preliminary experiment was first conducted to establish a process routine that produces fully dense, pore free and good metallurgically bonded deposit.

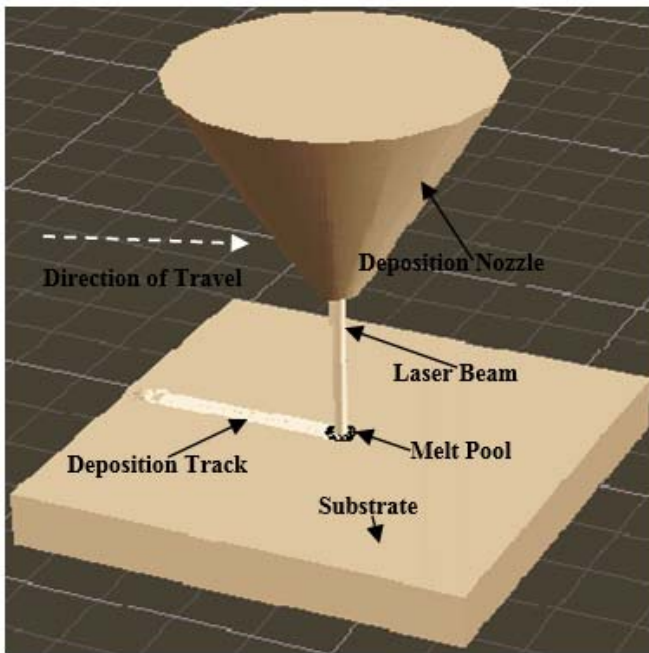


Fig. 2: Schematic view of laser metal deposition (LMD) process

Considering the result of the preliminary experiment, a laser power of 2000 W, scanning speed of 1 m/min, powder flow rate of 4 rpm and a gas flow rate of 2 l/min produced a fully dense, pore free with good metallurgical bonded deposit. These parameters were used as a benchmark in this study. The scanning speed, powder flow rate and the gas flow rate were fixed at these values and only the laser power was varied between 800 W and 2400 W. The processing parameters presented in this report are given as follow: Laser power, Scanning speed, Powder flow rate and Gas flow rate respectively.

The substrate was sandblasted and cleaned with acetone prior to the deposition process. A single track length of 90 mm was observed for the sample S1 to S8 while the length of 80mm was also observed for sample S9 were deposited for each of the processing parameter set in order to study the effect of the laser power changes on the evolving microstructure and the microhardness. The Table 1 presented the powder system with the corresponding mixing proportion.

TABLE I  
POWDERS WITH RESPECTIVE MIXING  
PROPORTION

Powders	Weight percentage (wt.%)	Flow rate (rpm)
Ti6Al4V	80	3.2
B <sub>4</sub> C	20	0.8

After the deposition process, the samples were laterally sectioned and mounted in resin. The samples were ground, polished and etched according to the standard metallographic preparation of Titanium. The samples were studied under the Optical Microscopy (OM). The microhardness characterization was performed on a digital Vickers hardness indenter. Thus, the polished samples were indented in which the indentations were carried out at a load setting of 500g and a dwell time of 15 seconds. However, the space between indentations was maintained at a distance of 10 $\mu$ m between each indentation throughout the hardness tests and at each interval ten indentations were taken and the average values were also recorded on each samples according to ASTM E384-11e1, 2011 [12].

### III. RESULTS AND DISCUSSION

The microstructure of the substrate used was observed under the optical microscope as shown in Figure 3. The microstructure is characterized by alpha and beta grain structure with the lighter part showing the alpha grains and the darker parts showing the beta grains. However, alpha phase dominates more grain structures than the beta phase and alpha phase was characterized by hard particles while the beta phase on the other hand characterized by the soft particles.

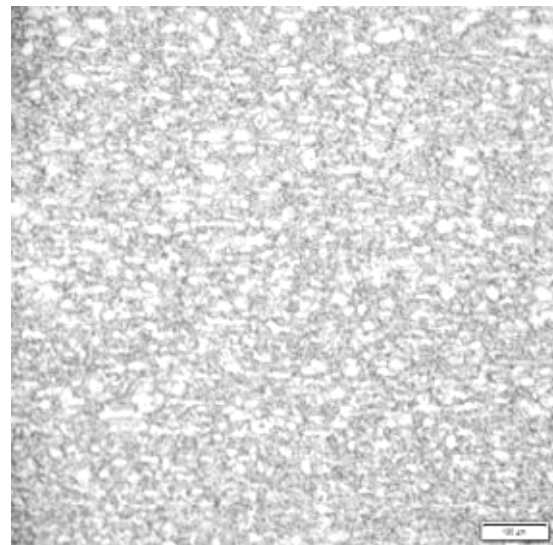


Fig. 3: Microstructure of the substrate

The schematic of the deposit as viewed from the cross-section is shown in Figure 4, it is divided into three microstructure zones. The deposit zone (DZ) consists of the melted deposited powder, the fusion zone (FZ) consists of the mixture of the substrate material and the deposited powder all melted and mixed to produce bonding of the deposited material with the substrate material. The heat affected zone (HAZ) on the other hand is the substrate material that has been heated up during the deposition process. The substrate acts as a heat sink and the part of the substrate that received high enough heat to cause microstructural changes in this area is referred to as the heat affected zone.

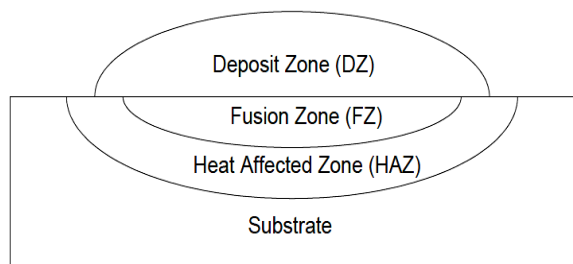


Fig. 4: Schematic view of the cross section of the deposit on the substrate

However, the results are divided into three parts namely: The physical appearance of the deposits, the microstructural characterization results, and the microhardness profiling results.

#### A. Physical appearance of the deposits

The physical appearance of the laser deposited composites ( $B_4C$ -Ti6Al4V) is illustrated in Figure 5. From the single track deposition showed, it was observed that the width of the deposit increased as the laser power increases. The microstructure of the surface was observed to have coarse and rough structure and gradually changes to fine and smooth surface structures as the laser power increases, the powders also characterized with a good deposit and a desirable melt pool during the deposition process as the laser power constantly increases. However, the bonding between the coating and the substrate appears physically good and their thickness also observed to be difference as the laser power increases from sample S1 to S9 respectively.

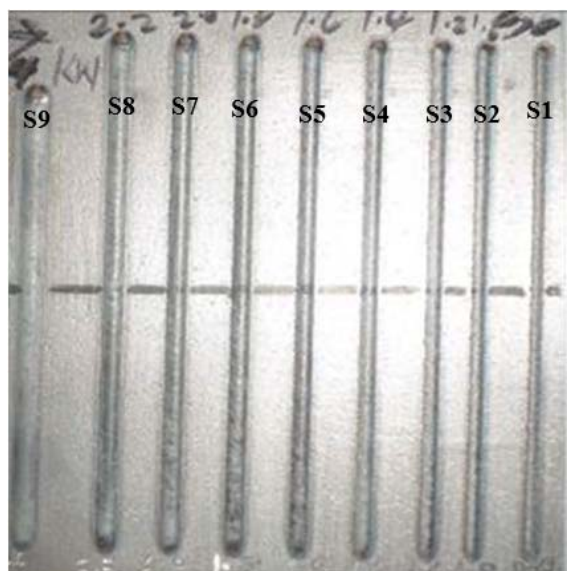


Fig. 5: Photograph of the deposited tracks of sample S1 to S9 on the substrate

The single track deposition of Figure 5 showed sample S1 to S9 with different parameter for each deposition in terms of laser power increasing from S1 to S9 (between 800 W to 2400 W) in which other parameters such as scanning speed, powder flow rate and gas flow rate were kept constant throughout the deposition.

#### B. Microstructural characterization

The microstructure of the substrate is characterized by the alpha and the beta phases as showed in Figure 3. The alpha phases are the light snow-flakes grain structures while the beta phases are the dark snow-flakes grain structures. However, the alpha phase dominates more grain structures than the beta phase and alpha phase was characterized by hard particles while the beta phase on the other hand was characterized by the soft particles. However, observation of the coating surface microstructure indicated the lamellar packing, which was associated with deposition process, oxidation was however occurs at the surface of the deposition. Thus, the micrograph of the sample S7 is shown in Figure 6 displaying the deposit zone, the fusion zone and the heat affected zone as depicted by the Figure 4. It can be observed that the grains are continuous from the fusion zone to the deposit zone and as well as the heat affected zone, and are martensitic structure, macroscopic banding and epitaxial in nature. These are seen apparently in all the samples and gradually become more profound as the laser power increases which is due to the presence of higher content of the titanium alloy (Ti6Al4V) when compared to the content of boron carbide particles involved in the deposition process. Thus, as showed in the Figure 7 (a) and (b) of sample S8 and S9 indicating both the epitaxial growth and the macroscopic banding that was observed in all the deposited samples.

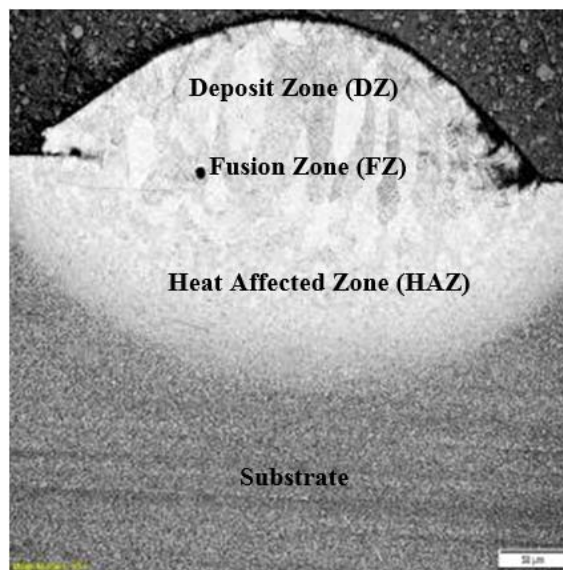


Fig. 6: Micrograph of laser deposited Ti6Al4V- $B_4C$  at a laser power of 2000 W showing the different zones

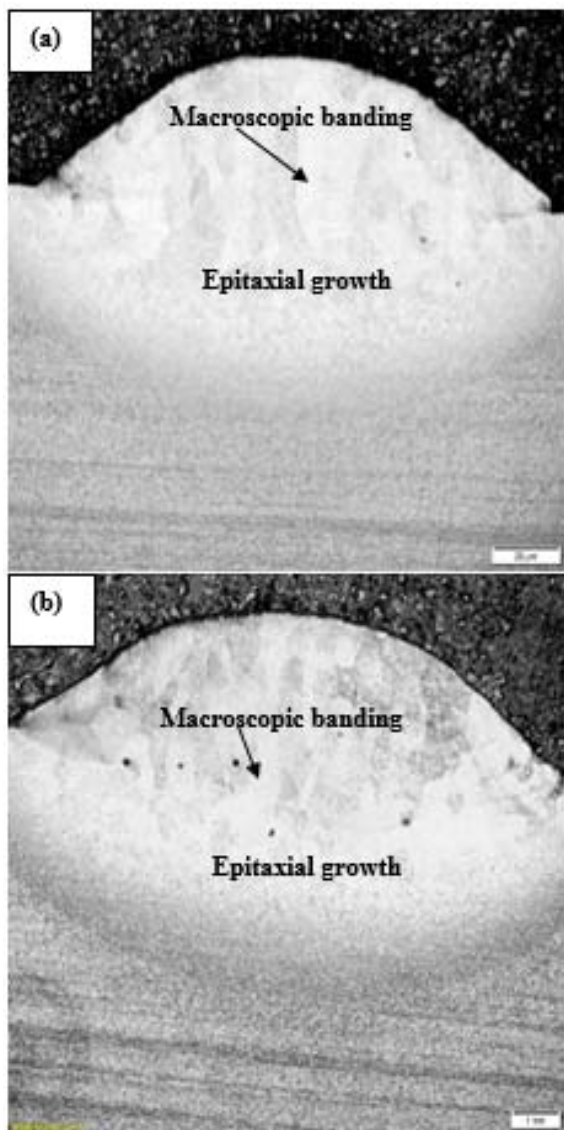


Fig. 7: Micrographs of laser deposited Ti6Al4V-B<sub>4</sub>C (a) Sample S8 deposited at a laser power of 2200 W; (b) Sample S9 deposited at a laser power of 2400 W

However, observation of the coating surface microstructure indicated the lamellar packing, which was associated with deposition process, oxidation was however occurs at the surface of the deposition. The level of homogeneity was observed as the laser power increases, the content of boron carbide particles in the composites were formed on the top layer of the deposit which actually behaves like a shielding structure or coated film-like structure on the deposition's surface. This property is however serves as the properties that is responsible for the resistance to wear as well as the corrosion due to the higher concentration of boron carbide particles deposited at the utmost surface of the deposit. Thus, [7] observed that, this property is characterized with the martensitic microstructure which shows a significant microhardness increase and corrosion resistance improvement.

The microstructure of the deposits was characterized by martensitic structure, basket weave- $\alpha$  and macroscopic banding observed to be associated with ductile properties of titanium alloy, Ti6Al4V. The Figures 8 and 9 presented the detailed characterization of these grain structures.

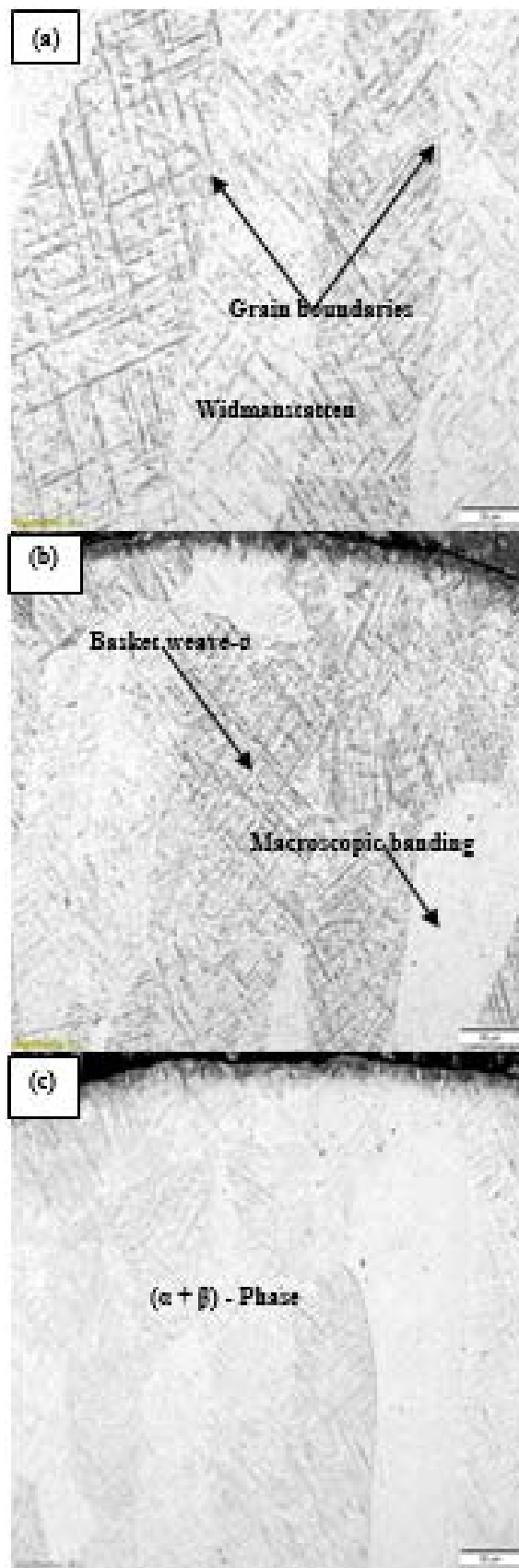


Fig. 8: Microstructures of laser deposited Ti6Al4V-B<sub>4</sub>C showing the grain structures (a) and (b) sample S7 deposited at a laser power of 2000 W; (c) sample S8 deposited at a laser power of 2200 W

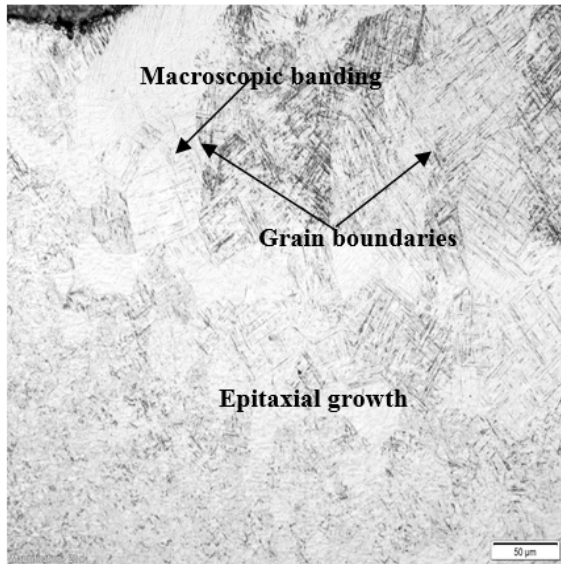


Fig. 9: Microstructure of sample S9 showing the grain structures

For other clarification, the micrographs revealed that, grain growths were observed on the heat affected zone and these were however attributed to the increase in the laser power. Furthermore, the basket weave martensitic structure which was presented in Figure 8 (a) and (b) resulting from heat input through laser metal deposition (LMD) process. Basket weave- $\alpha$  has however been known to benefit the mechanical properties of titanium alloy (Ti6Al4V). The Figure 8 (c) was however observed to be characterized with  $\alpha+\beta$  phase grain structure. Thus, the microscopic banding was observed to have an epitaxial growth on the globular microstructure which was shown in Figure 9 between the fusion zones (FZ) or the interface and the heat affected zone (HAZ) of the deposited composites.

### C. Microhardness profiling

The microhardness profiles of the composites were carried out on all the deposited samples from S1 to S9. Figure 10 presented the average Vickers hardness values together with their corresponding standard deviations. The Vickers microhardness values of the composites were however measured under a load of 500g at dwell time of 15 seconds on a digital microhardness tester. Prior to hardness measurements, the composites were sectioned, ground and polished by fine MD chem grinding disc with oxide polishing (OP-S) suspension to obtain a mirror-like finish on the surface in order to allow accurately measured indentations.

The Figure 10 presented that the hardness value increases as the laser power increases. However, at a certain instance, the hardness values decrease as the laser power increase and then the hardness value got to the peak and later decreases almost at constant hardness value as the laser power continue to increase. Therefore, sample S7 at a laser power of 2000 W was observed to have the highest hardness value. Thus, the variation in hardness values set as criteria to improve the ductility property of the composites. It is however observed that, increase in laser power influences the microstructure of the deposit which changes it from

rough and coarse surfaces smooth and fine surfaces which eventually tends to increase the hardness of the deposits. Nevertheless, it can be seen from the chart that the optimum laser power for the deposited composites were observed between 2000 W and 2400 W.

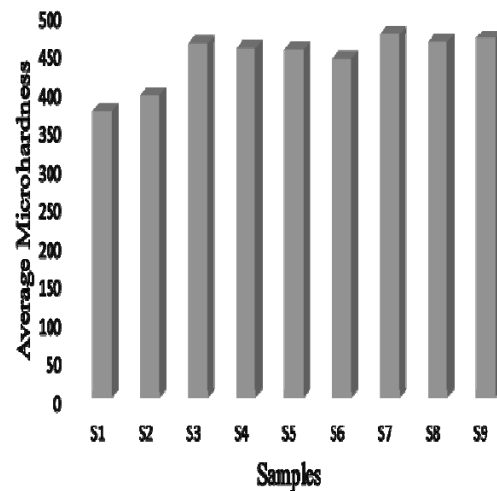


Fig. 10: Average Vickers microhardness profiles of the deposited composites

## IV. CONCLUSIONS

The study of the laser metal deposition of Ti6Al4V reinforced with  $B_4C$  particulate to improve the surface material properties was successfully achieved in this study. The surface effect of varying the laser power on the microstructure and the microhardness were extensively studied. The study revealed that laser processing parameters employed such as the laser power plays a very crucial role on the evolving properties of the deposits.

Microstructural analysis of the composites revealed that there were defect-free clads and good intermetallic phase of  $\alpha+\beta$  alloy with boron carbide ( $B_4C$ ). The sample S8 produced at a laser power of 2200 W was observed to be the best when compared to other samples deposited with respect to the intermetallic bonding and porosity-free. Furthermore, the microstructure of the heat affected zone ranged between fine and coarse globular primary alpha as the laser power increases. It was also observed that as the laser power increases, the microstructure ranged between fine martensite to coarse martensites. The average microhardness also increases with an increase in the laser power. It was however observed that the hardness was highly influenced by the laser power.

## REFERENCES

- [1] A. Jimoh. PhD Thesis: The Particulate-Reinforcement of Titanium Matrix Composites with Borides. The Faculty of Engineering and the Built Environment, University of the Witwatersrand, South Africa, 2010.
- [2] E. T. Akinlabi and S. A. Akinlabi. Characterization of Functionally Graded Commercially Pure Titanium (CPTI) and Titanium Carbide (TiC) Powders. In: Proceedings of the World Congress on Engineering, Vol. II, WCE, July 1-3, London, U.K, 2015.

- [3] R. M. Mahamood, E. T. Akinlabi, M. Shukla and S. Pityana. Characterization of Laser Deposited Ti6Al4V/TiC Composite Powders on a Ti6Al4V Substrate, *Lasers in Eng.* Vol. 29. Pp. 197-213, 2014.
- [4] R. M. Mahamood, E. T. Akinlabi, M. Shukla and S. Pityana. Effect of processing parameters on the properties of laser metal deposited Ti6Al4V using design of experiment, *IAENG Transactions on Engineering Sciences*, Taylor & Francis Group, London, ISBN 978-1-138-00136-7. pp. 331-339, 2014.
- [5] R. M. Mahamood, E. T. Akinlabi, M. Shukla and S. Pityana. Material Efficiency of Laser Metal Deposited Ti6Al4V: Effect of Laser Power, *International Association of Engineers, Engineering Letters*, 21:1, ISSN: 1816-093X (Print); 1816-0948 (Online), 2013.
- [6] R. M. Mahamood, E. T. Akinlabi, M. Shukla and S. Pityana. Scanning velocity influence on microstructure, microhardness and wear resistance performance of laser deposited Ti6Al4V/TiC composite, *Elsevier journal of Materials and Design* vol. 50, pp. 656-666, 2013.
- [7] F. Weng, C. Chen and Huijun Yu. Research status of laser cladding on titanium and its alloys: A review *journal of Materials and Design* vol. 58, pp. 412-425, 2014.
- [8] F. Thevenot. Boron Carbide: A comprehensive report: *Journal of the European Ceramic Society* vol. 6 pp. 205-225, 1990.
- [9] L. Levin, N. Frage and M. P. Dariel. A novel approach for the preparation of boron carbide-based cermets, *Elsevier international journal of refractory metals and hard materials* vol. 18, pp. 131-135, 2000.
- [10] S. Roy, A. Sarkar and S. Suwas. Characterization of deformation microstructure in Boron modified Ti-6Al-4V alloy. *Elsevier Journal of Materials Science and Engineering* vol. A528, pp. 449-458, 2010.
- [11] P. J. Arrazola, A. Garay, L. M. Iriarte, M. Armendia, S. Marya and F. Le Maitre. Machinability of titanium alloys (Ti6Al4V and Ti555.3). *Elsevier, a review journal of materials processing technology* vol. 209, pp. 2223-2230, 2008.
- [12] ASTM E384-11e1. Standard test method for Knoop and Vickers Hardness of materials, *ASTM international book of standards*, volume 03.01., 2011.